

Plasma Diagnosis from Thermal Noise and Limits on Dust Flux or Mass in Comet Giacobini-Zinner

N. MEYER-VERNET, P. COUTURIER, S. HOANG, C. PERCHE,
J. L. STEINBERG, J. FAINBERG, C. MEETRE

Thermal noise spectroscopy was used to measure the density and temperature of the main (cold) electron plasma population during 2 hours (1.5×10^5 kilometers perpendicular to the tail axis) around the point of closest approach of the International Cometary Explorer (ICE) to comet Giacobini-Zinner. The time resolution was 18 seconds (370 kilometers) in the plasma tail and 54 seconds (1100 kilometers) elsewhere. Near the tail axis, the maximum plasma density was 670 per cubic centimeter and the temperature slightly above 1 electron volt. Away from the axis, the plasma density dropped to 100 per cubic centimeter (temperature, 2×10^4 K) over 2000 kilometers, then decreased to 10 (1.5×10^5 K) over 15,000 kilometers; outside that region (plasma tail), the density fluctuated between 10 and 30 per cubic centimeter and the temperature between 1×10^5 and 4×10^5 K. The relative density of the hot population rarely exceeded a few percent. The tail was highly asymmetrical and showed much structure. On the other antenna, shot noise was recorded from the plasma particle impacts on the spacecraft body. No evidence was found of grain impacts on the antennas or spacecraft in the plasma tail. This yields an upper limit for the dust flux or particle mass, indicating either fluxes or masses in the tail smaller than implied by the models or an anomalous grain structure. This seems to support earlier suggestions that these grains are featherlike. Outside the tail, and particularly near 10^5 kilometers from its axis, impulsive noises indicating plasma turbulence were observed.

THIS REPORT SUMMARIZES THE RESULTS of an initial analysis of the radio experiment data during the International Cometary Explorer (ICE) encounter with comet Giacobini-Zinner. At the present stage of data reduction, there is no evidence that the experiment (1) detected any (nonlocal) radio emission from the comet. However, it recorded the electrostatic noise due to thermal motions of the plasma-charged particles. The spectroscopy of that noise yielded plasma parameters. These results were obtained with the 90-m (tip-to-tip) wire dipole antenna (S antenna); they are independent of the vehicle or antenna potential. The other antenna (Z antenna), which is a monopole, mostly recorded shot noise from the plasma-charged particles (and photoelectrons) impacting (or leaving) the spacecraft skin, and provides a measurement of spacecraft potential.

We found no evidence of dust impacts on the antenna or spacecraft; independent measurements with the two different antennas yielded the same quantitative upper limit of the dust flux or particle mass in the comet tail. Outside the plasma tail, the receiver recorded some additional noise, of which one sample is described here. This report

discusses only our method and results since a proper interpretation in terms of cometary physics requires a careful comparison between data from the different experiments on this spacecraft.

Deriving plasma parameters from the thermal noise spectrum. The thermal motion of the plasma-charged particles produced a fluctuating electric field (2) that is detected by the antenna-receiver system as thermal noise. In thermal equilibrium at temperature T , the noise spectrum is given (3) by the

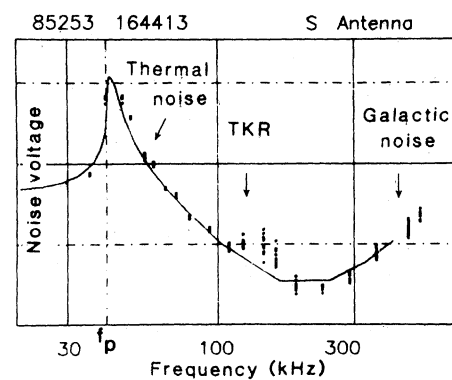


Fig. 1. Noise spectrum recorded on ICE, obtained by the long wire S antenna, on the eve of the encounter. It contains three components; thermal noise shows a clear cutoff at the plasma frequency f_p ; TKR is essentially sporadic and bursty; and galactic noise is only important at high frequencies. The continuous line is the best fit calculated spectrum (in its calculation, the galactic radiation has been slightly overestimated). The continuous horizontal line is at the $10^{-14} \text{ V}^2 \text{ Hz}^{-1}$ level at the receiver ports. The dashed and dotted lines are 10 dB apart.

Nyquist expression $V^2 = 4kTR$, where k is the Boltzman constant. The resistance R is the radiation resistance of the antenna in the plasma mode; this is because plasma waves are Landau-damped in the medium, which is thus "optically thick" for them. This resistance is much larger than the well-known resistance for electromagnetic waves; in any case, the latter do not play any role since the medium is generally "optically thin" for them. Therefore R depends on plasma wave emission and thus on both the plasma temperature T and density n . For space plasmas that are generally not in thermal equilibrium, this result can easily be generalized. For instance, when the plasma electron population can be represented by one cold and one hot component, with density and temperature n_c, T_c, n_h, T_h , the thermal noise spectrum is a more complicated function of these parameters (4-6). This function can generally be inverted to deduce those parameters from the spectrum.

We developed the necessary theory and computer software and applied the method to data acquired from ISEE-3 in the solar wind (5-8). Using that method requires only a sensitive and well-calibrated receiver mounted on an interference-free spacecraft, working in the proper frequency range with an antenna of the proper size. Our experiment, which was designed to study solar radio emissions, was only marginally suited to measure solar wind plasma parameters. But it happened, by chance, that it had the proper configuration for measuring plasma in the tail of comet Giacobini-Zinner.

The frequency of the plasma natural oscillations $f_p = 9 n^{1/2}$ kHz (n is the number density per cubic centimeter); this gives the time scale of the electron response to an electric perturbation. A second important parameter is the distance (Debye length) $L_D = 7 (T/n)^{1/2}$ m (T in electron volts) traveled by thermal electrons in the time $1/f_p$; this gives the scale length of the electric perturbation created by a static charge in the plasma. Since the electrons are not static, they support "plasma waves" that propagate at frequencies $f \approx f_p$ with a wavelength $\lambda \approx 2\pi\sqrt{3}L_D(1 - f_p^2/f^2)^{-1/2}$. At these frequencies, we "see" mostly the electrons, since the ions have a much larger time scale (by a factor of 200 for CO^+) (9).

These facts have several important consequences. For the receiver to be sensitive to the electron populations, it should operate at frequencies on the order of f_p (10). For $f < f_p$, a wire antenna "sees" the electrons that pass at a distance $r \approx L_D$ from its axis; the corresponding noise spectrum for an antenna of half-length $L \gg L_D$ is (11)

$$V^2 = 4 \times 10^{-13} T n^{-1/2} L^{-1} \text{ V}^2 \text{ Hz}^{-1} \quad (1)$$

N. Meyer-Vernet, P. Couturier, S. Hoang, C. Perche, J. L. Steinberg, Département de Recherche Spatiale, UA CNRS No. 264, Observatoire de Paris, 92195, Meudon, France.

J. Fainberg, Laboratory for Extraterrestrial Physics, NASA Goddard Space Flight Center, Greenbelt, MD 20771.

C. Meetre, Science Applications Research, 4400 Forbes Boulevard, Lanham, MD 20706.

(T in electron volts, n in number per cubic centimeter, L in meters). For $f \geq f_p$, the antenna couples to plasma waves. Since an antenna of length L is mostly sensitive to those waves of wavelength $\lambda \approx L$, the noise peaks at the frequency satisfying $\lambda(f) \approx L$; the larger L/L_D , the sharper the peak (5, 6). More precisely, whenever $L > \lambda$, the noise is (5, 6, 12)

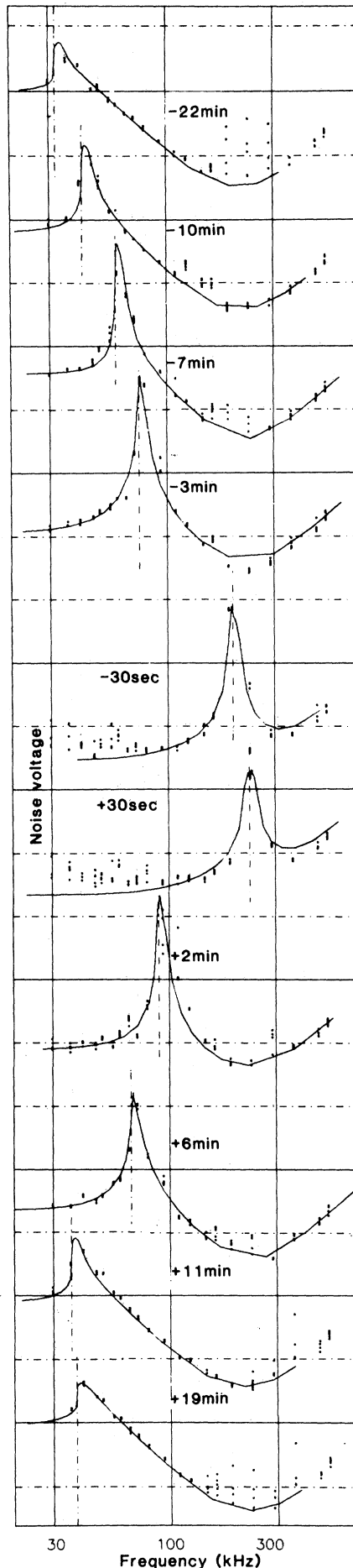
$$V^2 = \frac{6.5 \times 10^{-13} T n^{-1/2} L^{-1} (f_p/f)^3}{1 - (f_p/f)^2} \quad (2)$$

Thus, for $L/L_D \geq 1$, the spectrum exhibits a cutoff at the plasma frequency and a peak just above. For instance, with $L/L_D = 5$, the peak is at a frequency larger than $1.1f_p$ and its width (at half the peak level) is $0.3f_p$. Obtaining more general results often requires numerical computations. In particular, if there are suprathermal electrons (density n_h , temperature T_h), they interact mostly with plasma waves of phase velocity λf of the order of their mean velocity. This corresponds to much larger values of λ than for thermal electrons. Thus, broadly speaking, whenever $n_h \ll n_c$ the part of the spectrum very close to f_p yields n_h and T_h while the rest of it yields n_c and T_c . In practice, the finite receiver frequency resolution limits the accuracy of the measurements of the higher energy electrons.

Thus, an ideal thermal plasma detector should have a frequency range enclosing f_p and an antenna length much larger than L_D . The latter condition ensures, in addition, that the antenna will not be perturbed by the presence of the spacecraft (13). Another condition is that the thermal noise intensity be greater than other sources of noise (Fig. 1), particularly shot noise (which will be described below), galactic noise, terrestrial kilometric radiation (TKR), and receiver noise. All the above conditions were met during the ICE/Giacobini-Zinner encounter for the long wire antenna ($L = 45$ m) with a receiver frequency range 30 kHz to 2 MHz: the plasma frequency and Debye length (which are typically 30 kHz and 6 m in the solar wind) were 100 kHz and 1 m at 2000 km away from the tail axis and 230 kHz and 0.3 m at closest approach. In the worst situation, the minimum noise signal to be measured was still several times the receiver noise.

In this report only the total electron density ($n = n_c + n_h$) and the cold electron temperature (T_c) are given. The discussion

Fig. 2. A series of ten noise spectra recorded from 22 minutes before encounter to 19 minutes after. The layout and scales are the same as in Fig. 1. Note the drift of the cutoff frequency (f_p) due to the variation of the comet plasma density.



of n_h and T_h is deferred; the measurement of these parameters does not affect that of n , which stems unambiguously from the spectrum cutoff, and affects only weakly that of T_c since $n_h \ll n_c$.

Cold plasma density and temperature. Figure 2 shows several thermal noise spectra (14) recorded with the wire S antenna during the encounter. The data points are obtained as follows: the receiver frequency is programmed to change by steps; each step lasts 1.5 seconds (half of a spin period) over which five samples, 250 msec apart, are acquired from the S antenna (and one from the Z antenna). The frequency stepping sequence is not linear as a function of time: the higher frequency stepping rate is faster than the low-frequency one. For instance, the receiver tunes to 30 kHz every 54 seconds for 1.5 seconds, but tunes to 188 kHz every 18 seconds, also for 1.5 seconds. The five dots in Fig. 2, for each frequency channel, are obtained by interpolation. The continuous curves correspond to the theoretical thermal noise spectrum (plus, at high frequencies, the galactic noise) calculated with the set of parameters n_c , T_c , n_h , and T_h that gives the best fit to the minima observed on each frequency channel; in that way, we eliminate data points that are clearly associated with nonthermal noise. In every case, we find $n_h \ll n_c \approx n$. In the fitting process, we could easily discard TKR, which is very "bursty" and appears on some spectra near 250 kHz. Note that the spectra obtained 20 minutes (25,000 km) before and after closest approach are not very different from those obtained on the day before encounter (Fig. 1).

Figure 3 shows the cold plasma density and temperature obtained by fitting such spectra over 54-second (or shorter) intervals from 1 hour (7.5×10^4 km) before to 1 hour after closest approach. When it is not limited by the time resolution, the quality of the fit with so few free parameters ensures a precision better than 10 percent on n_c and 30 percent on T_c in the tail.

During this period the measured plasma parameters varied as follows: outside the tail, density fluctuated between 10 and 30 cm^{-3} and temperature fluctuated between 1×10^5 and 4×10^5 K on a typical scale of 2 minutes, which is still larger than our coarsest time resolution. Defining the plasma tail as the high-density and low-temperature region, we find that it had an extent of about 20 minutes (30,000 km), was asymmetrical, and had several density peaks. The most outstanding peak occurred at closest approach where the density was 670 cm^{-3} (temperature, 13,000 K) and decreased to 100 cm^{-3} in less than 2 minutes (2500 km).

Figure 4 shows n_c and T_c in the tail with a

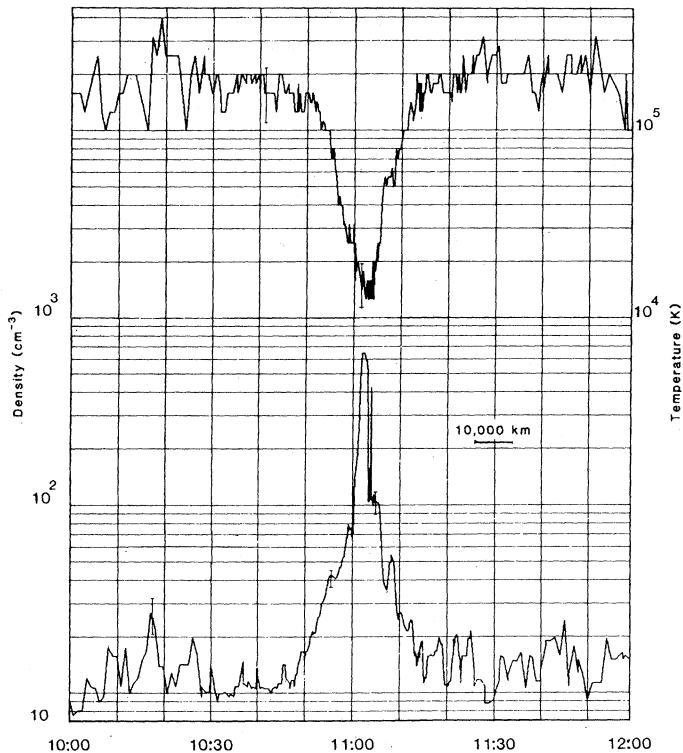


Fig. 3. Variation of the plasma density (bottom) and temperature (top) during encounter deduced from several hundred fits similar to those in Fig. 2. The central part is expanded in Fig. 4. The error bars, which vary with the density, are only typical ones. The ICE trajectory passes at 7800 km from the nucleus with a relative velocity of 20.7 km sec⁻¹.

resolution of 18 seconds (370 km). This improvement in resolution was made possible because, as explained above, the higher frequencies of the receiver are sampled more frequently than the lower ones.

In some cases a large noise variation (up to a factor of 50) was observed within one 1.5-second frequency step; this is interpreted as meaning that that particular channel was sampled while the steep cutoff of the noise spectrum was moving across the channel bandwidth; then we are sure that the cutoff frequency (f_p) lay inside the received frequency band, which was 3 or 10 kHz wide depending on the channel at the time of observation, and thus within the 1.5-

second duration of a frequency step. This confirms, in more detail, the existence of the peaks shown in Fig. 3. In particular, the peak $n = 427 \text{ cm}^{-3}$ at 11:03:59 U.T. would not have been seen if the plasma frequency had not crossed three successive receiving channels at the right times. Except in those examples, we cannot exclude variations on a time scale much shorter than 18 seconds (370 km). Note also that we cannot discriminate between spatial and temporal variations.

Electron shot noise. The plasma thermal noise discussed above is due to electrons passing near the antenna, at distance $\leq L_D$ for $f < f_p$ or $< \lambda$ for $f > f_p$. Actually, some

particles hit the antenna surface and the surface emits photoelectrons. In the present range of parameters this effect can be approximated (15, 16) by adding a shot noise component $V^2 = \sum_j N_j e^2 |Z|^2 / 2$ (e is the electron charge, Z the antenna impedance, and N_j the number of independent events j per unit time). Using current balance and standard approximate expressions for the ambient electron flux (17) and the antenna (radius a) capacitance (12), we get for $f/f_p < 1$ and $a \ll L_D \ll L$ (15): $V^2 = 2.2 \times 10^{-14} (a/L) T^{1/2} [Ln(a/L_D)]^2 (f_p/f)^2 f(\varphi) \text{ Hz}^{-1}$ (18), where T is in electron volts, φ is the ratio of the antenna direct current potential to T , and $f(\varphi)$ stands for the variation of the electron flux with φ ; if $\varphi \ll 1$, $f(\varphi) \approx 1 + \varphi$; if $\varphi < 0$, $f(\varphi) = e^\varphi$.

This effect contributes very little to the noise on the S antenna in our frequency range except in the narrow high-density region near the tail axis. There, it gives a highly spin-modulated component: when the antenna is parallel to the sun's direction, the plasma electron current is balanced only by the ion current, yielding $f(\varphi) \ll 1$, while in the perpendicular direction, $f(\varphi)$ is on the order of 1. This accounts for the lower frequency noise on the two spectra acquired near the tail axis in Fig. 2.

This argument does not consider molecule impacts. These induce electron and ion secondary emission, which can contribute to the noise (19). At the flyby velocity, the kinetic energy of molecules is small (typically 40 eV for H₂O or 100 eV for CO₂). Thus, secondary emission of electrons is expected to be negligible (20); the yield γ_i for secondary emission of ions (due mostly to sputtering) is poorly known. Taking $\gamma_i \approx 2 \times 10^{-3}$ (21), we find that this effect is smaller than that of the cometary electron flux if the density of molecules at encounter is smaller than 10^7 cm^{-3} . With the present estimates of the gas production rate in comet Giacobini-Zinner at encounter time, this inequality holds.

The above discussion was concerned with the wire dipole antenna in the spin plane. The other antenna is made of two short booms parallel to the spin axis. It was not well suited to measure plasma parameters, and one of the booms was in the spacecraft wake during encounter. Thus, we decided to switch off the preamplifier of that boom in order to get a monopole working against the spacecraft and to detect particle impacts on the latter. Owing to the large area of the spacecraft, that antenna mostly detects shot noise due to electron and ion impacts and photoelectron ejection. By comparing the data (Fig. 5) with theoretical calculations (using the plasma parameters obtained from the S-antenna spectrum), we can measure

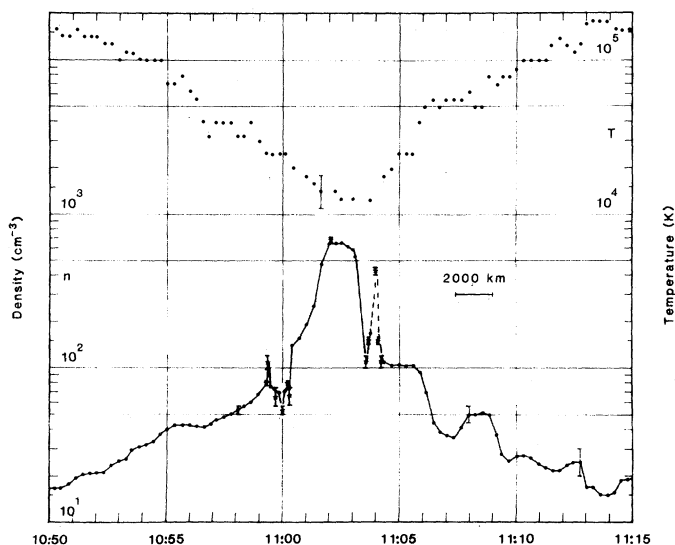


Fig. 4. Plasma density (bottom) and temperature (top) across the comet tail (resolution, 18 seconds or 380 km). The thick vertical bars on the density profile indicate the points where a 1.5-second time resolution is obtained.

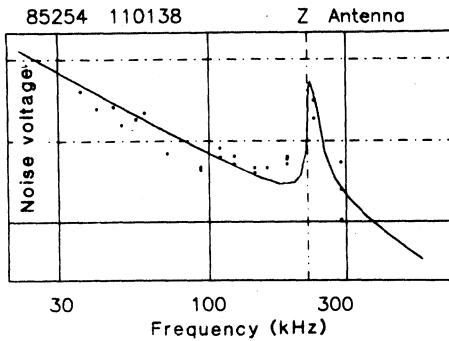


Fig. 5. Noise spectrum of the Z antenna taken 1 minute before closest approach. It is essentially made of thermal noise (mostly above f_p) and impact noise (below f_p). The latter component is a function of the spacecraft potential, which has been set for best fit of the theoretical spectrum (continuous line) to the data (dots). The horizontal continuous straight line is at the level $10^{-16} \text{ V}^2 \text{ Hz}^{-1}$. The dashed and dotted lines are 10 dB apart.

the spacecraft potential, which is an important quantity for those experiments counting low-energy particles approaching the spacecraft. A preliminary evaluation gives a slightly negative value (-1 to -2 V) at encounter.

No evidence of dust grain impacts in the tail. When Voyager 2 crossed Saturn's ring plane, both the radio astronomy receiver (22) and the plasma wave instrument (23) recorded noise due to dust impacts, well above the thermal and shot plasma noise level.

The outstanding characteristic of the data acquired with the S antenna during the 20-minute comet tail crossing is that they almost perfectly fit theoretical plasma noise spectra. In other words, they show no evidence of dust impacts. Likewise, the Z antenna results are in agreement with the interpretation in terms of shot noise due to plasma particle impacts on and photoelectron emission from the spacecraft; they show no evidence of any other source of noise. This absence of dust detection can yield upper limits of the grain flux or mass in the plasma tail if one makes a few hypotheses concerning the grain-antenna interaction.

When a small dust grain hits the antenna or spacecraft at 21 km/sec, it is vaporized and ionized; this produces an expanding plasma cloud, and a fraction of the charge Q is recollected. The amplitude of the recorded voltage depends on Q , which is a function of the grain mass m ; its time variation (the squared Fourier transform of which is the spectrum) depends on the dynamics of the cloud and charge recollection, which itself depends on the ambient plasma.

The S antenna is an almost perfectly symmetrical dipole; thus, it should be much

more sensitive to impacts on the antenna itself than to those on the spacecraft, even though the latter are much more numerous (by a factor of 100). Indeed, the voltage detected by the antenna is the difference between the voltages induced on the two symmetrical wires; thus the voltage detected after an impact on the spacecraft is at most equal to the voltage due to an impact on the antenna itself multiplied by the ratio of the spacecraft diameter to the antenna length ($\approx 1/45$). Therefore, the ratio of the contributions to the noise spectrum is at most $1/45^2$ for one impact or $100/45^2 \ll 1$ if there are many impacts during one individual measurement. Thus, impacts on the spacecraft should contribute negligibly to the noise on the S antenna. For the charge Q , we use, as a first step, the usual empirical expressions together with laboratory data (24). Taking, as a conservative estimate, a factor of 10 below these values yields $Q \approx 10^{-3} m^{0.8}$ (with Q in Coulombs and m in grams). Assuming a step function time variation (18), this yields a shot noise spectrum analogous to the plasma shot noise, but where the electron charge e is replaced by Q ; an integral over the mass distribution should be made if there are many grain impacts during an individual measurement.

With these parameters, one impact of a 10^{-10} -g grain during an individual (0.125-second) measurement yields a noise level much higher than that of plasma noise (10^3 times at 30 kHz near the tail axis) and the galactic noise (below 300 kHz). Let us assume for instance one impact per second of such grains on the S antenna [this is of the same order as the numbers obtained from earlier models (25)]. Then on each spectrum, such as those shown in Fig. 2, one should see about 11 data points (26) well above the rest of the data (10^3 times higher at 30 kHz). Such an impact rate is clearly excluded. This figure can be lowered by examining all the data acquired during the 20 minutes of closest approach: at frequencies below 100 kHz and during that period of time, there is no data point above the plasma noise level, while a 10^{-10} -g grain impact should be above it by a factor of 10^3 at 30 kHz. These data were acquired during 8 percent of the time, that is, during 96 seconds. This gives an upper limit on the order of 10^{-2} per second for the impact rate of grains with mass $m \geq 10^{-10}$ g on the antenna. Owing to the projected surface ($3.5 \times 10^{-2} \text{ m}^2$) and relative velocity, this gives an upper limit on the order of 10^{-5} m^{-3} for the mean density of these grains in the plasma tail.

Let us now discuss the Z-antenna monopole, which records impacts on the spacecraft itself (projected surface 100 times larg-

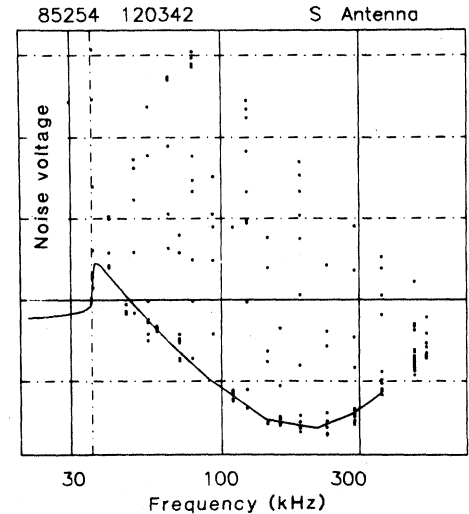


Fig. 6. Example of the spectra that show short spikes much more intense than thermal noise, recorded on the long wire S antenna around 1 hour (70,000 km) before and after closest approach. Layout and scales are the same as in Fig. 1. The fit of the theoretical spectrum (continuous line) is poor unless made to the lowest data points.

er than that of the S antenna). In that case, both the rise time of the signal due to one impact (plasma cloud expansion and recollection) and that of the discharge due to the plasma and photoelectron currents play an important role in determining the noise spectrum (18). A preliminary calculation yields a noise due to one impact (10^{-10} -g grain) in an individual measurement (1.5 seconds) of the same order as the plasma thermal and shot noise level (Fig. 5). Since there is no data point above the plasma noise level, there could possibly be one impact per measurement but not much more. This yields a maximum impact rate on the spacecraft of nearly 1 sec^{-1} , which is equivalent, owing to the surface ratio, to that found above for the S antenna.

We thus obtain an upper limit for the impact rate about 100 times smaller than predicted by the models (25). The fact that this limit is provided by two independent measurements (impacts on the antenna and on the spacecraft, independently) gives much weight to this result. Note that the noise spectral density varies as the charge squared, thus approximately as mass to the power 1.6. Therefore, a much larger quantity of smaller grains, as for instance one grain per cubic meter with a mass of 10^{-13} g or a mass distribution yielding the same noise level, cannot be excluded. In addition, we cannot provide any limit outside the plasma tail, since the spectra are not sufficiently quiet (Fig. 6). This preliminary estimate could be refined by using a more correct modelling of the rain-target interaction

and of the grain mass distribution function. But the present results could suggest, for instance, that comet Giacobini-Zinner has very low density grains ("feathers"), in agreement with previous deductions from Giacobinid-meteor observations (25).

Impulsive noise. On several occasions, outside the plasma tail, particularly from 1 hour 30 minutes to 1 hour (1.0×10^5 to 0.7×10^5 km) before encounter and from 45 minutes to 1 hour (0.5×10^5 to 0.7×10^5 km) after, the S antenna recorded a noise much above (10 to 10^3 times) the thermal noise level. Figure 6 shows an example. These spectra, which could indicate a high level of turbulence, are reminiscent of data acquired in Earth's magnetosheath; their study has only been started. The presence of this noise prevents us from setting any limit on dust impacts outside the plasma tail.

REFERENCES AND NOTES

- R. Knoll *et al.*, *IEEE Trans. Geosci. Electron.* GE-16, 199 (1978).
- A. G. Sitenko, *Electromagnetic Fluctuations in Plasma* (Academic Press, New York, 1967).
- O. De Pazzis, *Radio Sci.* 4, 91 (1969); A. Andronov, *Kosm. Issled.* 4, 558 (1967).
- J. A. Fejer and J. R. Kan, *ibid.* 4, 721 (1969).
- N. Meyer-Vernet, *J. Geophys. Res.* 84, 5373 (1979).
- P. Couturier, S. Hoang, N. Meyer-Vernet, J. L. Steinberg, *ibid.* 86, 11127 (1981); in *Solar Wind 5*, A. J. Lazarus and M. Neugebauer, Eds. (NASA Publ. 2280, Woodstock, 1983), pp. 377-383.
- S. Hoang *et al.*, *J. Geophys. Res.* 85, 3419 (1980).
- N. Meyer-Vernet, P. Couturier, S. Hoang, J. L. Steinberg, R. D. Zwickl, *ibid.*, in press.
- Except if the bulk plasma velocity in the antenna frame induces an important Doppler shift (8).
- This discussion neglects the ambient static magnetic field. If $L/L_D \gg 1$, this requires that the electron gyrofrequency and its lowest harmonics be much smaller than f_c [P. Meyer and N. Vernet, *Radio Sci.* 9, 409 (1974); D. T. Nakatani and H. H. Kuehl, *ibid.* 11, 433 (1976); D. D. Sentman, *J. Geophys. Res.* 87, 1455 (1982)].
- H. H. Kuehl, *Radio Sci.* 1, 971 (1966).
- K. G. Balmain, *J. Res. Natl. Bur. Stand.* D69, 559 (1965).
- If the spacecraft size is smaller or of the order of L_D .
- All the spectra shown in this report were measured or calculated at the receiver input ports. They are related to the noise spectrum V^2 at the antenna terminals by the transfer gain calculated (7) from the receiver and antenna impedances.
- N. Meyer-Vernet, *J. Geophys. Res.* 88, 8081 (1983).
- M. Petit, *Ann. Telecommun.* 30, 351 (1975).
- J. G. Lafframboise and L. W. Parker, *Phys. Fluids* 16, 629 (1973).
- The f^{-2} spectrum assumes that f^{-1} is both smaller than the system time constant and larger than the rise time of the signal; this condition generally holds for the wire S antenna; but it does not hold everywhere for the Z antenna. This also neglects the contribution of the photoelectrons recollected after emission.
- R. J. L. Grard, in *Proc. 17th ESLAB Symp.* (ESA SP-198, 1983), pp. 151-159.
- Since the energy is too low for kinetic emission to occur (D. T. Young, *ibid.*, pp. 143-150).
- This estimation is rather hazardous [R. Schmidt and H. Arends, in *Proc. GIOTTO PEW Meet.* (ESA SP-224, 1984), pp. 15-19, 22].
- M. G. Aubier, N. Meyer-Vernet, B. M. Pedersen, *Geophys. Res. Lett.* 10, 5 (1983).
- D. A. Gurnett, E. Grün, D. Gallagher, W. S. Kurth, F. L. Scarf, *Icarus* 53, 236 (1983).
- F. R. Krüger and J. Kissel, in *Proc. GIOTTO PEW Meet.* (ESA SP-224, 1984), pp. 43-48; E. Grün, *ibid.*, pp. 39-41.
- N. Divine, JPL Interoffice Memorandum 5137-84-164 (Jet Propulsion Laboratory, Pasadena, CA, 1984). D. K. Yeomans and J. C. Brandt, *The Comet Giacobini-Zinner Handbook* (Jet Propulsion Laboratory, Pasadena, CA, 1985).
- With an impact rate of 1 sec^{-1} , the probability of an impact for each 0.125-second measurement is 0.125. There are 18 frequency channels below 300 kHz, with five data points each. This yields $0.125 \times 18 \times 5 \approx 11$ points.
- We are grateful to the team of engineers and technicians, spread on both sides of the Atlantic and led by R. Knoll, who designed, built, tested, and integrated our instrument and made it the most sensitive one ever flown; it is thanks to their hard work, dedication, and competence that we could systematically use the weak thermal noise ($10^{-14} \text{ V}^2 \text{ Hz}^{-1}$ is only $4.5 \text{ } \mu\text{V}$ in our 3-kHz bandwidth) as a powerful plasma diagnosis tool. Our thanks are also due to the ISEE-3 project team in NASA-GSFC and to the Fairchild team who succeeded in designing, building, and testing a very quiet spacecraft. The French part of the experiment was financed under contract with Centre National d'Etudes Spatiales.

20 November 1985; accepted 4 February 1986

Ion Composition Results During the International Cometary Explorer Encounter with Giacobini-Zinner

KEITH W. OGILVIE, M. A. COPLAN, P. BOCHSLER, J. GEISS

The International Cometary Explorer spacecraft passed through the coma of comet Giacobini-Zinner about 7800 kilometers antisunward of the nucleus on 11 September 1985. The ion composition instrument was sensitive to ambient ions with mass-to-charge ratios in the ranges 1.4 to 3 atomic mass units per electron charge ($\text{amu } e^{-1}$) and 14 to 33 $\text{amu } e^{-1}$. Initial interpretation of the measurements indicates the presence of H_2O^+ , H_3O^+ , probably CO^+ and HCO^+ , and ions in the mass range 23 to 24; possible candidates are Na^+ and Mg^+ . In addition to these heavy ions, measured over the velocity range 80 to 223 kilometers per second, the instrument measured He^{2+} of solar wind origin over the range 237 to 463 kilometers per second. The heavy ions have a velocity distribution which indicates that they have been picked up by the motional electric field, whereas the light ions are steadily decelerated as the comet tail axis is approached. These results are in agreement with the picture of a comet primarily consisting of water ice, together with other material, that sublimates, streams away from the nucleus, becomes ionized, and interacts with the solar wind.

SPECTROSCOPIC OBSERVATIONS OF the comas of comets (1-3) have indicated the presence of various ionic species. Mass spectrometric measurements of ions in the coma of comet Giacobini-Zinner were made during the encounter of the International Cometary Explorer (ICE) on 11 September 1985, when the spacecraft passed within 7800 km of the nucleus on its antisunward side. For mass-to-charge (M/Q) ratios from 14 to 33 $\text{amu } e^{-1}$, H_2O^+ was the dominant ion; several other species were also detected.

Observations at Venus (4) and at Titan (5), where flowing plasma interacts directly with a dense atmosphere, have established the modification of the plasma flow field by the formation of ions that picked up momentum from the plasma. The same phenomenon was predicted to occur on a much larger scale in comets (6). For Giacobini-Zinner the measurements by the ion composition instrument (ICI) of the velocity distributions of He^{2+} ions, which are diagnostic of the flow field, combined with measurements of the distributions of heavy ions from the comet, confirmed the prediction.

The ICI (7, 8) was designed for solar wind measurements and was used to study the composition of the solar wind and the velocity distributions of and velocity differ-

ences among solar wind ions (9). The ions in the solar wind are highly charged since they retain the charge states acquired in the corona; the appropriate range of values of M/Q normally covered by the ICI was 1.4 to 5.8 $\text{amu } e^{-1}$, measured over a solar wind velocity (V) range of 300 to 620 km sec^{-1} . The ranges of M/Q and V in which observations were made were set by parameters read into the instrument microprocessor through the spacecraft command system. To cover values of M/Q and V appropriate to the comet (where singly charged ions are expected), a set of parameters was found that selected 14 M/Q values between 14 and 33 $\text{amu } e^{-1}$ for V between 80 to 224 km sec^{-1} and 14 M/Q values between 1.4 and 3 $\text{amu } e^{-1}$ for V between 237 and 463 km sec^{-1} . The dual M/Q range was achieved by causing an overflow condition in the microprocessor calculating the potentials applied to the plates of the energy analyzer, which forms part of the ICI, in a way similar to that used to study ions in Earth's magnetic tail (10). The overflow took place for V

K. W. Ogilvie, NASA/Goddard Space Flight Center, Code 692, Greenbelt, MD 20771.

M. A. Coplan, Institute for Physical Science and Technology, University of Maryland, College Park, MD 20742.

P. Bochsler and J. Geiss, Physikalisches Institut, University of Bern, 3012 Bern, Switzerland.